Korean J. Chem. Eng., 33(1), 248-254 (2016)
DOI: 10.1007/s11814-015-0129-4

pISSN: 0256-1115
eISSN: 1975-7220

Vapor-liquid equilibria for the binary mixtures of dimethyl ether (DME)+ dimethyl carbonate (DMC)

Wan Ju Jeong and Jong Sung Lim†

Department of Chemical and Biomolecular Engineering, Sogang University, C. P. O. Box 1142, Seoul 100-611, Korea
(*Received 5 February 2015 • accepted 13 June 2015*)

Abstract−Isothermal vapor-liquid equilibrium data for the binary system of dimethyl ether (DME)+dimethyl carbonate (DMC) were measured at 303.15, 313.15, 323.15, 333.15 and 343.15 K using a circulation-type equilibrium apparatus with on-line gas chromatography analysis. The experimental data were correlated with the Peng-Robinson equation of state (PR-EoS) using the van der Waals one fluid mixing rule and the Peng-Robinson equation of state (PR-EoS) using the Wong-Sandler mixing rule combined with the NRTL excess Gibbs free energy model. This system showed negative deviation from Raoult's law, and no azeotropic behavior was observed for all the temperature ranges studied here. Calculated results with PR-EoS using both two mixing rules showed good agreement with experimental data.

Keywords: Vapor Liquid Equilibria, Dimethyl Ether (DME), Dimethyl Carbonate (DMC), Peng-Robinson Equation of State (PR-EoS)

INTRODUCTION

Dimethyl carbonate (DMC) has attracted much attention as a non-toxic substitute for dimethyl sulfate, methyl halide and phosgene, which are toxic and corrosive agents in methylation and carbonylation reactions. DMC is quickly biodegradable and does not have irritating or mutagenic effects by physical contact and inhalation, so it is not harmful to humans and the environment. Furthermore, it has been used as a fuel additive for improving the octane number instead of MTBE, an electrolyte in lithium batteries and a starting material for the synthesis of various chemical products [1-7].

There are various existing methods for synthesis of DMC: (1) phosgene route, (2) the oxidative carbonylation of methanol with carbon monoxide and oxygen that was introduced by EniChem [8], and (3) methyl nitrite that was introduced by UBE [9]. However, the aforementioned processes require materials that are toxic, explosive and flammable gases such as phosgene, hydrogen chloride and carbon monoxide. Also, these routes have not only the problem that that they are harmful to the environment, but also many drawbacks such as corrosion of equipment and difficulty of separation process among the products.

Recently, direct synthesis of DMC from supercritical carbon dioxide and methanol has been suggested. DMC can be synthesized by the reaction of methanol with carbon dioxide, and simultaneously dimethyl ether (DME) and water are generated as by-product. Unlike other methods using or producing toxic chemicals, this method contains environmentally benign and thermodynamically stable compounds. In addition, it is more attractive due to the low cost of reactants [10-13]. Many studies focused on improving DMC yield have been carried out under the various experimental conditions. The results showed that the DMC selectivity in direct synthesis method is influenced by many factors such as temperature, pressure, acidity, reaction time and catalysts [14-16]. As mentioned above, DME is produced as by-product caused by methanol dehydration. So, to increase DMC selectivity and decrease DME selectivity, it is important to find the optimum experimental condition. Therefore, vapor liquid equilibrium data of materials associated with the direct synthesis method are necessary for determining optimal reaction condition and designing the optimum separation process. For these reasons, we have studied for many years the phase equilibria of binary systems related to the direct synthesis of DMC, such as, DME+Methanol [17], DMC+CO_2 [18], DME+CO_2 [19], CO_2+CH_3I [20], and DME+CH_3I [21] systems in series.

In this work, isothermal VLE data for the binary mixture of DME (1)+DMC (2) at five equally spaced temperatures from 303.15 to 343.15 K were measured by using a circulation-type equilibrium apparatus in which both phases were continuously recirculated. The experimental data were correlated with the Peng-Robinson equation of state [22] using the van der Waals mixing rule [23,24] and the Peng-Robinson equation of state using the Wong-Sandler mixing rule [25] combined with the NRTL excess Gibbs free energy model [26]. In addition, the average absolute deviations of pressure and vapor phase compositions between experimental and calculated values were reported, and the relevant parameters were determined.

EXPERIMENTAL

1. Chemicals

High-grade chemicals of DME and DMC were used for the VLE measurement. DME was purchased from Sigma Aldrich (USA) (greater than 99.0 mass %), and DMC was purchased from Samchun Chemicals (KOREA) (greater than 99.9 mass %). We ana-

†To whom correspondence should be addressed.
E-mail: limjs@sogang.ac.kr

Table 1. Thermodynamic properties of components [28]

Chemical	Chemical formula	T_C/K	P_C/MPa	ω	Purity (mass %)
Dimethyl ether (1)	C_2H_6O	400.1	5.370	0.2002	≥99.0
Dimethyl carbonate (2)	$C_3H_6O_3$	557.0	4.800	0.3360	≥99.5

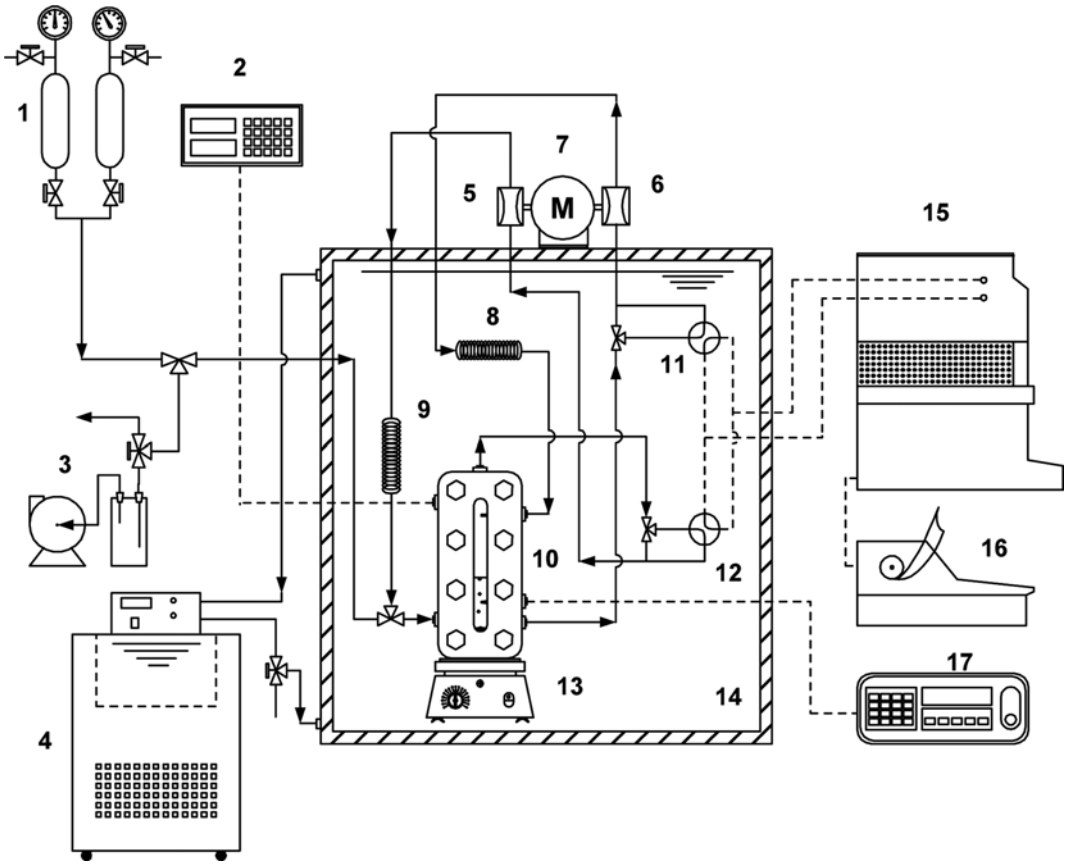

Fig. 1. Schematic diagram of the experimental apparatus.

1. Sample reservoir
2. Pressure indicator
3. Vacuum pump
4. Bath circulator
5. Vapor circulation pump
6. Liquid circulation pump
7. Electric motor
8. Liquid/liquid heat exchanger
9. Gas/liquid heat exchanger
10. Equilibrium cell
11. Liquid auto-sampler
12. Vapor auto-sampler
13. Magnetic stirrer
14. Bath containing heat carrier
15. Gas chromatograph
16. Computing integrator
17. Temperature indicator

lyzed these two pure components by gas chromatography (GC). The resulting purities of DME and DMC were higher than 99.5 and 99.9 mass %, respectively. So, they were used without any further purification. The purity data and properties of these components are shown in Table 1.

2. Experimental Apparatus

A schematic diagram of the experimental apparatus for measuring VLE data in this study is shown in Fig. 1. The vapor-liquid equilibrium apparatus used in this work is the same as that used in our previous work [17-21]. It is a circulation-type equilibrium apparatus in which both liquid and vapor phases were recirculated continuously. The equilibrium cell is a type-316 stainless steel vessel within an inner volume of about 85 cm^3. In its middle part, two Pyrex glass windows of 20 mm thickness were installed front and back so that the liquid level, mixing and circulating behaviors, and critical phenomena could be observed by a back light during operation. A stirrer, rotated at variable speeds by an external magnet, was used to accelerate the attainment of the equilibrium state and to reduce concentration gradients in both phases.

The temperature of the equilibrium cell in the water bath was maintained by a circulator, Haake model AC150 from Fisher Scientific Ltd., UK. The temperature in the cell was measured with a platinum-resistance sensor and a digital temperature indicator model F200 precision thermometer from Automatic Systems Laboratories, Ltd., UK. They were calibrated by the National Measurement Accreditation Service accredited calibration laboratory. The total uncertainty in temperature measurements is estimated to be within 0.01 K, including sensor uncertainty, temperature resolution, 0.001 K, and measurement uncertainty, 0.001 K. The pressure was measured with a pressure transducer, Model XPM60, and a digital pressure

calibrator, Model PC106, from Beamex, Finland. Pressure calibrations are traceable to National Standards (Center for Metrology and Accreditation Cert. No. M-95P077, 14.11.1995, M-M 730, 16.11.1995, and M-95P078, 16.11.1995). The calibrator uncertainty was 0.0005 MPa, the sensor uncertainty was 0.001 MPa, and the measurement uncertainty was 0.001 MPa. Therefore, the total uncertainty of the pressure measurement is estimated to be within 0.001 MPa.

The vapor and liquid phases in the equilibrium cell were continuously recirculated by a dual-head circulation pump from the Milton Roy Company to reach the equilibrium state rapidly in the cell. The composition of the phases was determined by means of a gas chromatograph, model YL6100 from Young-Lin Instrument Co., Korea, connected online to the VLE cell. The response of the thermal-conductivity detector (TCD) was carefully calibrated using the mixture prepared gravimetrically and the GC with a Porapak Q column from Alltech Company. Data derived from gas chromatography were treated with a computer program (Autochro-WIN from Young-Lin Instrument Co., Korea).

3. Experimental Procedure

Experiments to measure VLE data for the binary system of (DME (1)+DMC (2)) were performed using the following procedures. The system was first evacuated to remove all inert gases. A certain amount of DMC was supplied to the cell, and then the temperature of the entire system was held constant by controlling the temperature of the water bath. After the desired temperature was attained, the pressure of the pure component was measured. A certain amount of DME was introduced into the cell from a sample reservoir. Both the vapor and liquid phases were recirculated by a dual-head circulation pump until an equilibrium state was established. Two hours were sufficient to obtain thermal equilibrium between the cell fluid and the thermostatic bath as well as between the vapor and liquid phases. After equilibration was reached, the pressure in the equilibrium cell was measured, and then vapor and liquid samples were withdrawn from the recycling lines by the vapor and liquid sampling valves, respectively. The compositions of the samples were measured by immediately injecting them into the GC, which was connected online to the vapor and liquid sampling valves. The GC was calibrated with pure components of known purity and with mixtures of known composition that were prepared gravimetrically. At least five analyses were performed for each phase, and the average values were considered to correspond to the equilibrium values. Considering the margin of error and the reproducibility of the GC, we estimated an overall uncertainty of 0.002 in the measurements of the mole fraction for both the liquid and the vapor phases.

CORRELATION

1. Correlation with the PR-EoS using the Van der Waals Mixing Rule

The experimental VLE data were correlated with the Peng-Robinson equation of state (EOS) [22] using Van der Waals one fluid mixing rules [23,24].

$$P = \frac{RT}{v_M - b} - \frac{a(T)}{v_M(v_M + b) + b(v_M - b)} \tag{1}$$

$$a(T) = 0.457235\frac{R^2T_c^2}{P_c}\alpha(T) \tag{2}$$

$$b = 0.077796\frac{RT_c}{P_c} \tag{3}$$

$$\alpha(T) = [1 + k(1 - \sqrt{T/T_c})]^2 \tag{4}$$

$$k = 0.37464 + 1.54226\omega - 0.26992\omega^2 \tag{5}$$

where the parameter a is a function of temperature, b is constant, k is a constant characteristic of each substance, ω is the acentric factor, P (MPa) is the pressure, P_c (MPa) is the critical pressure, T (K) is the absolute temperature, T_c (K) is the critical temperature, and v_M is the molar volume of the mixture.

The van der Waals one fluid mixing rules were used in this work to obtain EoS parameters for a mixture from those of the pure components. These mixing rules for a cubic equation of state can be written as follows:

$$a_m = \sum_i\sum_j x_i x_j a_{ij} \tag{6}$$

$$b_m = \sum_i\sum_j x_i x_j b_{ij} \tag{7}$$

Where

$$a_{ij} = (1 - k_{ij})a_i^{1/2}a_j^{1/2} \tag{8}$$

$$b_{ij} = \frac{b_i + b_j}{2}(1 - \eta_{ij}) \tag{9}$$

The binary interaction parameters (k_{ij} and η_{ij}) were obtained by minimizing the following objective function:

$$\text{Objective Function} = \frac{1}{N}\sum_i^N\left[\left(\frac{P_{j,exp} - P_{j,cal}}{P_{j,exp}}\right) \times 100\right]^2 \tag{10}$$

where N is the number of experimental data points and P_{exp} and P_{cal} are the experimental and the calculated pressures, respectively.

2. Correlation with the PR-EoS using the W-S Mixing Rule

The experimental VLE data were correlated with the PR-EoS [22] using the Wong-Sandler mixing rule [25].

$$b_m = \frac{\Sigma_i\Sigma_j x_i x_j (b - a/RT)_{ij}}{(1 - A_\infty^E/CRT - \Sigma_i x_i a_i/RTb_i)} \tag{11}$$

with

$$(b - a/RT)_{ij} = \frac{1}{2}[(b - a/RT)_i + (b - a/RT)_j](1 - k_{ij}) \tag{12}$$

and

$$\frac{a_m}{b_m} = \sum_i x_i\frac{a_i}{b_i} + \frac{A_\infty^E}{C} \tag{13}$$

where C is a numerical constant equal to $\ln(\sqrt{2}-1)/\sqrt{2}$ for the Peng-Robison EoS used in this work. The single adjustable parameter (k_{ij}) for each binary pair is referred to as the Wong-Sandler mixing rule parameter. Also, A_∞^E is an excess Helmholtz free energy model at infinite pressure that can be equated to a low-pressure excess Gibbs energy model [26]. In this study, the nonrandom two-liquid (NRTL) model [27] was used and is given in the following equations:

$$\frac{A_{\infty}^{E}}{RT}=\sum_{i}x_i\frac{\Sigma_j x_j G_{ji}\tau_{ji}}{\Sigma_r x_r G_{ri}} \quad (14)$$

with

$$G_{ji}=\exp(-\alpha_{ji}\tau_{ji}) \quad \text{and} \quad \tau_{ji}=(g_{ji}-g_{ii})/RT \quad (15)$$

We have set the non-randomness parameter, α_{ij} equal to a fixed value of 0.3 for all of the binary mixtures studied here. Pure component parameters T_c, P_c, and ω, necessary for calculating the a and b values of the pure components of interest in this study, are shown in Table 1.

RESULTS AND DISCUSSION

The isothermal VLE data for the DME (1)+DMC (2) binary systems were measured at five temperatures ranging from 303.15 to 343.15 K at 10 K intervals. In Table 2, the comparisons of measured vapor pressures of pure DME and DMC with the calculated values from NIST Standard Reference Database 103b [28] are presented. The measured pure component data are considered to be reliable and consistent with available literature data. The average of the relative deviations ($\Sigma|\Delta P/P|/N$ (%)) between the measured and calculated vapor pressure was 0.51% for DME and 1.86% for DMC, respectively. In Table 3, the experimental vapor-liquid equilibrium data and the results of the correlation are listed. This table contains the measured equilibrium pressure and mole fractions of the vapor and liquid phases for each temperature and the calculated pressure and mole fraction of the vapor composition. In addition, relative deviations between measured and calculated pressures ($|\Delta P/P_{exp}|$) and vapor compositions ($|\Delta y/y|$) are represented.

Table 2. Comparison of the measured pure component vapor pressures with literature data [28]

Component	T/K	P_{exp}/MPa	P_{ref}/MPa	$\lvert\Delta P\rvert$	$\lvert\Delta P\rvert/P_{exp}$
Dimethyl ether (1)	303.15	0.689	0.681	0.009	0.013
	313.15	0.898	0.891	0.007	0.008
	323.15	1.144	1.146	0.001	0.001
	333.15	1.456	1.450	0.005	0.004
	343.15	1.812	1.811	0.000	0.000
			Ave	0.005	0.005
Dimethyl carbonate (2)	303.15	0.010	0.009	0.000	0.040
	313.15	0.016	0.015	0.001	0.035
	323.15	0.024	0.023	0.000	0.009
	333.15	0.035	0.035	0.000	0.001
	343.15	0.051	0.051	0.000	0.008
			Ave	0.000	0.019

Fig. 2 shows a comparison of the measured and calculated values with the PR-EoS using the van der Waals one fluid mixing rule and PR-EoS using the W-S mixing rule for the binary system of DME (1)+DMC (2) at various temperatures 303.15, 313.15, 323.15, 333.15 and 343.15 K. As can be seen, the calculated values using both mixing rules are in close accordance with the experimental data. This binary mixture system showed no azeotropic behavior and slightly negative deviation from Raoult's law.

In Table 4, the interaction parameters, the adjustable binary parameters k_{ij}, the average relative deviations of the pressure (ARD-P (%)), and the average relative deviations of the vapor-phase composition (ARD-y (%)) of the binary mixtures between the measured and

Table 3. Vapor-liquid equilibrium measurements for DME (1)+DMC (2) system

Experimental data			PR EOS (VdW)/NRTL				PR EOS (W-S)/NRTL			
P_{exp}/MPa	$x_{1,exp}$	$y_{1,exp}$	P_{cal}/MPa	$y_{1,cal}$	[a]ΔP/P (%)	[b]Δy/y (%)	P_{cal}/MPa	$y_{1,cal}$	[a]ΔP/P (%)	[b]Δy/y (%)
T=303.15 K										
0.010	0.000	0.000	0.010	0.000	1.956	0.000	0.010	0.000	1.956	0.000
0.116	0.233	0.939	0.125	0.937	7.990	0.247	0.123	0.938	6.590	0.145
0.198	0.362	0.970	0.199	0.965	0.252	0.467	0.199	0.967	0.491	0.254
0.282	0.495	0.981	0.284	0.980	0.743	0.130	0.287	0.982	1.914	0.074
0.355	0.602	0.986	0.360	0.987	1.358	0.168	0.365	0.989	2.843	0.331
0.429	0.716	0.988	0.448	0.993	4.315	0.474	0.454	0.994	5.776	0.579
0.557	0.862	0.990	0.568	0.997	1.993	0.728	0.573	0.998	2.825	0.765
0.629	0.951	0.991	0.642	0.999	2.066	0.804	0.644	0.999	2.358	0.813
0.689	1.000	1.000	0.682	1.000	1.123	0.000	0.682	1.000	1.123	0.000
T=313.15 K										
0.016	0.000	0.000	0.015	0.000	1.861	0.000	0.015	0.000	1.861	0.000
0.144	0.219	0.934	0.141	0.909	1.418	2.681	0.139	0.910	3.154	2.561
0.264	0.391	0.969	0.265	0.960	0.319	1.015	0.266	0.963	0.613	0.688
0.345	0.490	0.978	0.347	0.973	0.733	0.474	0.351	0.976	1.783	0.168
0.474	0.626	0.980	0.477	0.985	0.553	0.550	0.484	0.988	2.123	0.770
0.587	0.737	0.983	0.595	0.992	1.428	0.905	0.604	0.993	2.985	1.040
0.714	0.862	0.984	0.737	0.997	3.322	1.303	0.745	0.997	4.371	1.354
0.809	0.948	0.991	0.836	0.999	3.319	0.833	0.840	0.999	3.736	0.845
0.898	1.000	1.000	0.894	1.000	0.470	0.000	0.894	1.000	0.470	0.000

Table 3. Continued

Experimental data			PR EOS (VdW)/NRTL				PR EOS (W-S)/NRTL			
P_{exp}/MPa	$x_{1,exp}$	$y_{1,exp}$	P_{cal}/MPa	$y_{1,cal}$	[a]ΔP/P (%)	[b]Δy/y (%)	P_{cal}/MPa	$y_{1,cal}$	[a]ΔP/P (%)	[b]Δy/y (%)
T=323.15 K										
0.024	0.000	0.000	0.024	0.000	0.372	0.000	0.024	0.000	0.372	0.000
0.200	0.210	0.923	0.202	0.902	0.652	2.208	0.200	0.904	0.018	2.027
0.338	0.341	0.963	0.337	0.950	0.426	1.362	0.338	0.952	0.116	1.147
0.523	0.495	0.979	0.517	0.974	1.222	0.459	0.520	0.976	0.498	0.291
0.676	0.626	0.981	0.681	0.985	0.759	0.490	0.682	0.987	0.827	0.608
0.820	0.737	0.987	0.822	0.991	0.267	0.484	0.816	0.992	0.404	0.558
0.962	0.858	0.989	0.971	0.996	0.889	0.681	0.960	0.996	0.212	0.714
1.068	0.952	0.991	1.087	0.999	1.743	0.732	1.079	0.999	1.065	0.740
1.144	1.000	1.000	1.151	1.000	0.594	0.000	1.151	1.000	0.594	0.000
T=333.15 K										
0.035	0.0000	0.0000	0.035	0.000	1.025	0.000	0.035	0.000	1.025	0.000
0.223	0.2040	0.8880	0.226	0.869	1.565	2.136	0.223	0.869	0.108	2.084
0.425	0.3610	0.9454	0.421	0.942	0.810	0.380	0.426	0.944	0.387	0.098
0.618	0.4824	0.9574	0.600	0.967	2.838	0.952	0.608	0.969	1.543	1.216
0.843	0.6356	0.9718	0.852	0.983	1.062	1.200	0.852	0.985	1.083	1.381
1.056	0.7699	0.9821	1.079	0.992	2.116	0.995	1.066	0.993	0.927	1.096
1.253	0.8885	0.9873	1.273	0.997	1.560	0.937	1.256	0.997	0.266	0.979
1.381	0.9659	0.9906	1.400	0.999	1.341	0.853	1.392	0.999	0.775	0.863
1.456	1.0000	1.0000	1.461	1.000	0.360	0.000	1.461	1.000	0.360	0.000
T=343.15 K										
0.051	0.0000	0.0000	0.051	0.000	0.224	0.000	0.051	0.000	0.224	0.000
0.200	0.1195	0.7961	0.202	0.764	0.901	4.024	0.199	0.761	0.544	4.396
0.410	0.2685	0.9081	0.406	0.895	1.057	1.469	0.406	0.896	1.114	1.341
0.736	0.4768	0.9509	0.732	0.953	0.579	0.200	0.742	0.955	0.722	0.419
1.052	0.6532	0.9744	1.055	0.976	0.331	0.122	1.073	0.977	1.981	0.280
1.277	0.7673	0.9810	1.290	0.985	1.042	0.460	1.309	0.986	2.486	0.562
1.539	0.8872	0.9866	1.558	0.994	1.299	0.716	1.571	0.994	2.138	0.757
1.704	0.9584	0.9898	1.727	0.998	1.301	0.800	1.732	0.998	1.625	0.812
1.812	1.0000	1.0000	1.828	1.000	0.892	0.000	1.828	1.000	0.892	0.000

[a]$\Delta P/P\ (\%)=(P_{exp}-P_{cal})/P_{exp}|\times 100$

[b]$\Delta y/y\ (\%)=|(y_{exp}-y_{cal})/y_{exp}|\times 100$

Total uncertainty of the temperature is within 0.01 K

Total uncertainty of the pressure is within 0.001 MPa

Overall uncertainty of liquid and vapor phase mole fraction is within 0.002

Table 4. Values of binary parameters and average relative deviations of P and y

T/K	PR EOS (VdW)				PR EoS (W-S)				
	[a]k_{12}	η_{12}	[c]ARD-P (%)	[d]ARD-y (%)	[a]k_{12}	[b]τ_{12}	[b]τ_{21}	[c]ARD-P (%)	[d]ARD-y (%)
303.15	−0.0364	−0.1367	2.422	0.335	−0.0429	−0.2476	−0.2476	2.875	0.329
313.15	−0.0506	−0.1652	1.491	0.862	−0.0578	−0.3089	−0.3089	2.344	0.825
323.15	−0.0407	0.0795	0.769	0.713	−0.0449	−2.8995	−0.3540	0.456	0.676
333.15	−0.0591	0.0918	1.409	0.828	−0.0685	−4.0666	2.5920	0.719	0.857
343.15	−0.0340	−0.0956	0.847	0.866	−0.0387	0.0001	0.0001	1.303	0.952
Ave	−0.0442		1.388	0.721	−0.0505			1.539	0.728

[a]k_{12}, [b]τ_{12} and [b]τ_{21} is dimensionless

[b]NRTL: $\tau_{12}=(g_{12}-g_{22})/RT$, $\tau_{21}=(g_{21}-g_{11})/RT$

[c]$\text{ARD-P}\ (\%)=(1/N)\Sigma|(P_{exp}-P_{cal})/P_{exp}|\times 100$

[d]$\text{ARD-y}\ (\%)=(1/N)\Sigma|(y_{exp}-y_{cal})/y_{exp}|\times 100$

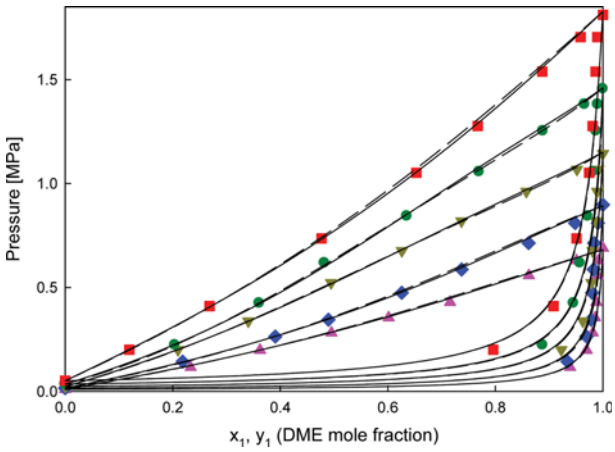

Fig. 2. P-x-y diagram for the DME (1)+DMC (2) system. Experimental data at various temperatures: ▲, 303.15 K; ◆, 313.15 K; ▼, 323.15 K; ●, 333.15 K; ■, 343.15 K; —, calculated with the PR EoS using VdW mixing rule; ---, calculated with the PR EoS using W-S mixing rule.

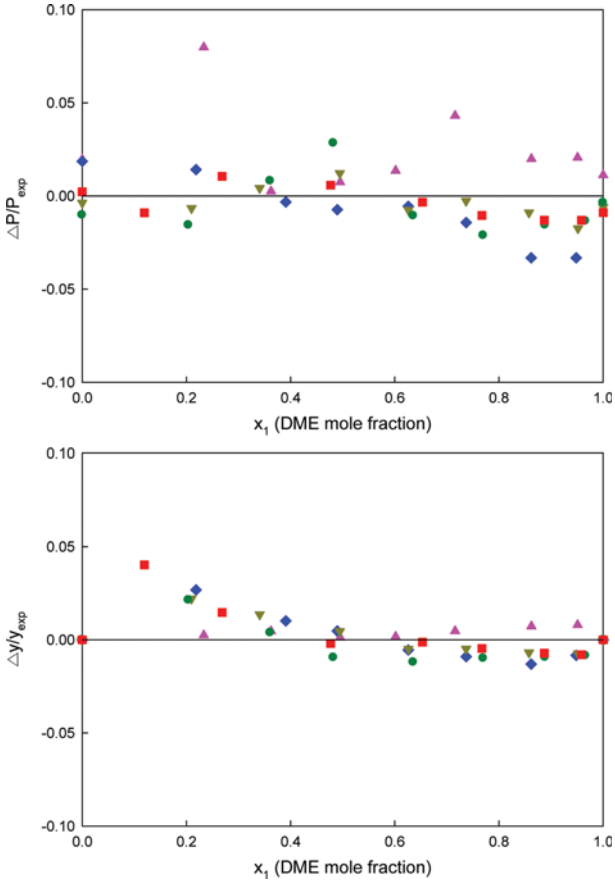

Fig. 3. Deviation of pressure and vapor composition for the system of DME (1)+DMC (2) from the PR- EoS using VdW mixing rule: ▲, 303.15 K; ◆, 313.15 K; ▼, 323.15 K; ●, 333.15 K; ■, 343.15 K.

calculated values are listed. The overall average values of ARD-P (%) and ARD-y (%) through the temperature range from 303.15

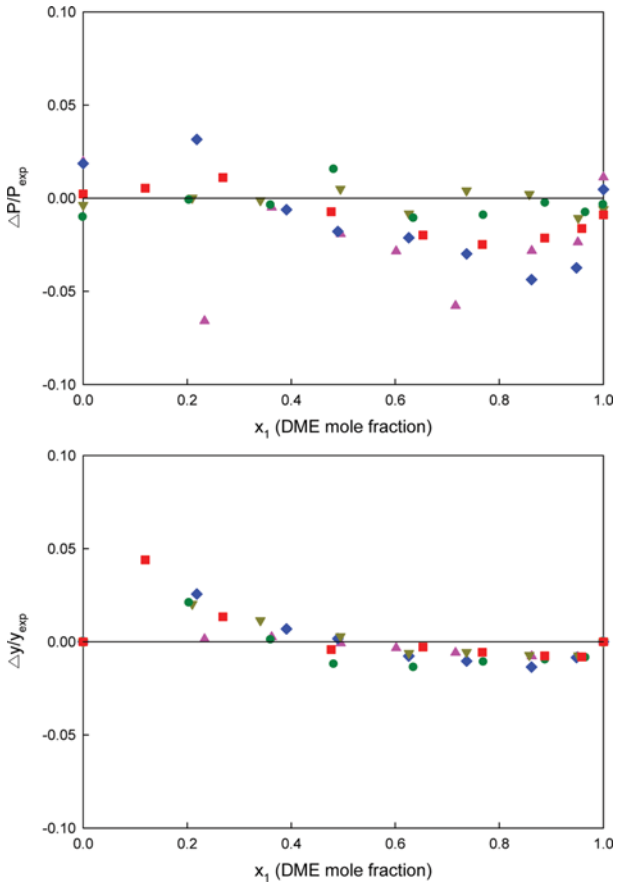

Fig. 4. Deviation of pressure and vapor composition for the system of DME (1)+DMC (2) from the PR- EoS using W-S mixing rule: ▲, 303.15 K; ◆, 313.15 K; ▼, 323.15 K; ●, 333.15 K; ■, 343.15 K.

to 343.15 K were 1.3877% and 0.7208% for the PR-EoS using the one fluid mixing rule and 1.4855% and 0.7279% for the PR-EoS using the W-S mixing rule, respectively. ARD-P (%) and ARD-y (%) values calculated with the one fluid mixing rule are rather smaller than those of the W-S mixing rule, but the differences are not big, so both can be considered suitable to estimate the experimental data.

In Figs. 3 and 4, the relative deviations of pressure ($\Delta P/P_{exp}$) and the vapor phase compositions ($\Delta y_1/y_{exp}$) for the PR-EoS using the one fluid mixing rule and the PR-EoS using the W-S mixing rule are plotted with the liquid phase compositions (x_1), point by point. From these figures and the low average deviations of P and y, we conclude that the calculated values with the PR-EoS using both mixing rules give good agreement with the experimental data.

CONCLUSION

The isothermal vapor-liquid equilibrium data for the binary systems of dimethyl ether (DME)+dimethyl carbonate (DMC) were measured at five equally spaced temperatures of 303.15, 313.15, 323.15, 333.15, and 343.15 K by using a circulation-type equilibrium apparatus. The experimental VLE data were correlated with the PR-EoS using the van der Waals one fluid mixing rule and the

PR-EoS using the Wong-Sandler mixing rule. This binary system showed negative deviations at each temperature, and showed no azeotropic behavior. The average relative deviations of the pressures and the vapor-phase compositions showed that the PR-EoS using the one fluid mixing rule had somewhat better correlation with the experimental data than the PR-EoS using W-S mixing rule. But the differences were small, so both mixing rules can be considered suitable to estimate the experimental data.

NOMENCLATURE

a(T) : attraction parameter (temperature dependent) [MPa cm^6 mol^{-2}]
b : molecular volume parameter [cm^3mol^{-1}]
P, P_c : pressure, critical pressure [MPa]
R : gas constant 8.3144 [$J \cdot mol^{-1} K^{-1}$]
k_{ij} : interaction parameter
T, T_c : absolute temperature, critical temperature [K]
v_M : molar volume [cm^3mol^{-1}]
x : liquid mole fraction
y : vapor mole fraction
A_∞^E : excess Helmholtz free energy at infinite pressure [J mol^{-1}]
G, g : excess Gibbs energy [$J \cdot mol^{-1}$]

Greek Letters

ω : acentric factor
α : non-randomness parameter

Subscripts

c : critical property
cal : calculated
exp : experimental
i, j : i th, j th component of the mixture
r : reduced property

REFERENCES

1. P. Tundo and M. Selva, *Accounts Chem. Res.*, **35**, 706 (2002).
2. Y. Ono, *Appl. Catal. A-Gen.*, **155**, 133 (1997).
3. M. A. Pacheco and C. L. Marshall, *Energy Fuel*, **11**, 2 (1997).
4. Y. Ono, *Catal. Today*, **35**, 15 (1997).
5. A.-A. G. Shaikh and S. Sivaram, *Chem. Rev.*, **96**, 951 (1996).
6. Y. Ein-Eli, *Electrochem. Commun.*, **4**, 644 (2002).
7. D. Delledonne, F. Rivetti and U. Romano, *Appl. Catal. A-Gen.*, **221**, 241 (2001).
8. U. Romano, R. Tesel and M. M. Mauri, *Ind. Eng. Chem. Prod. Res. Dev.*, **19**, 396 (1980).
9. T. Matsuzaki and A. Nakamura, *Catal. Surv. Asia*, **1**, 77 (1997).
10. S. Fang and K. Fujimoto, *Appl. Catal. A-Gen.*, **142**, L1 (1996).
11. C. Li and S. Zhong, *Catal. Today*, **82**, 83 (2003).
12. S. T. Hong, H. S. Park, J. S. Lim, Y. W. Lee, M. Anpo and J. D. Kim, *Res. Chem. Intermed.*, **32**, 737 (2006).
13. S. T. Hong, H. S. Park, J. S. Lim and K. P. Yoo, *Korean Chem. Eng. Res.*, **46**, 550 (2008).
14. K. Tomishige, T. Sakaihori, Y. Ikeda and K. Fujimoto, *Catal. Lett.*, **58**, 225 (1999).
15. K. Almusaiteer, *Catal. Commun.*, **10**, 1127 (2009).
16. K. Tomishige and K. Kunimori, *Appl. Catal. A-Gen.*, **237**, 103 (2002).
17. S. A. Kim, J. H. Yim, H. S. Byun and J. S. Lim, *Korean J. Chem. Eng.*, **28**, 2324 (2011).
18. M. H. Lee, J. H. Yim, J. W. Kang and J. S. Lim, *Fluid Phase Equilib.*, **318**, 77 (2012).
19. M. H. Lee, J. H. Yim and J. S. Lim, *Korean J. Chem. Eng.*, **29**, 1418 (2012).
20. H. Cho, J. H. Yim and J. S. Lim, *J. Supercrit. Fluids*, **81**, 7 (2013).
21. H. Cho, J. E. Kim and J. S. Lim, *Fluid Phase Equilib.*, **379**, 52 (2014).
22. D.-Y. Peng and D. B. Robinson, *Ind. Eng. Chem. Fundam.*, **15**, 59 (1976).
23. S. K. Shibata and S. I. Sandler, *Ind. Eng. Chem. Res.*, **28**, 1893 (1989).
24. J. Im, M. Kim, J. Lee and H. Kim, *J. Chem. Eng. Data*, **49**, 243 (2004).
25. D. S. H. Wong and S. I. Sandler, *AIChE J.*, **38**, 671 (1992).
26. D. S. Abrams and J. M. Prausnitz, *AIChE J.*, **21**, 116 (1975).
27. H. Renon and J. M. Prausnitz, *AIChE J.*, **14**, 135 (1968).
28. M. Frenkel, R. D. Chirico, V. Diky, C. D. Muzny and A. F. Kazakov, NIST ThermoData Engine, NIST Standard Reference Database 103b-Pure Compounds, Binary Mixtures, and Chemical Reactions, Version 5.0, Standard Reference Data Program, National Institute of Standards and Technology, Gaithersburg, MD (2010).